ARTreat Project: Three-Dimensional Numerical Simulation of Plaque Formation and Development in the Arteries

Nenad Filipovic, *Member, IEEE*, Mirko Rosic, Irena Tanaskovic, Zarko Milosevic, Dalibor Nikolic, Nebojsa Zdravkovic, Aleksandar Peulic, Milos R. Kojic, Dimitris I. Fotiadis, *Senior Member, IEEE*, and Oberdan Parodi

Abstract—Atherosclerosis is a progressive disease characterized by the accumulation of lipids and fibrous elements in arteries. It is characterized by dysfunction of endothelium and vasculitis, and accumulation of lipid, cholesterol, and cell elements inside blood vessel wall. In this study, a continuum-based approach for plaque formation and development in 3-D is presented. The blood flow is simulated by the 3-D Navier–Stokes equations, together with the continuity equation while low-density lipoprotein (LDL) transport in lumen of the vessel is coupled with Kedem-Katchalsky equations. The inflammatory process was solved using three additional reaction–diffusion partial differential equations. Transport of labeled LDL was fitted with our experiment on the rabbit animal model. Matching with histological data for LDL localization was achieved. Also, 3-D model of the straight artery with initial mild constriction of 30% plaque for formation and development is presented.

Index Terms—Atherosclerosis, low-density lipoprotein (LDL), plaque, wall shear stress.

I. INTRODUCTION

ATHEROSCLEROSIS is a progressive disease characterized in particular by the accumulation of lipids and fibrous

N. Filipovic is with the Faculty of Mechanical Engineering, University of Kragujevac, 34000 Kragujevac, Serbia (e-mail: fica@kg.ac.rs).

A. Peulic is with Technical Faculty Cacak, University of Kragujevac, 32000 Cacak, Serbia (e-mail: apeulic@sbb.rs).

M. Rosic, I. Tanaskovic, and N. Zdravkovic are with the Faculty of Medicine, University of Kragujevac, 34000 Kragujevac, Serbia (e-mail: mrosic@medf.kg.ac.rs; irena.vuk@gmail.com; nzdravkovic@gmail.com).

Z. Milosevic D. Nikolic are with Bioengineering Research and Development Center, 34000 Kragujevac, Serbia (e-mail: zarko@kg.ac.rs; markovac85@kg.ac.rs).

M. Kojic is with the Methodist Hospital System, Houston, TX 77030 USA, with the Harvard School of Public Health, Boston, MA 02115 USA, and also with the Bioengineering Research and Development Center, 34000 Kragujevac, Serbia (e-mail: mkojic@hsph.harvard.edu).

D. I. Fotiadis is with University of Ioannina, 45110 Ioannina, Greece (e-mail: fotiadis@cs.uoi.gr).

O. Parodi is with CNR Clinical Physiology Institute, Via Moruzzi 1, Pisa 56124, Italy (e-mail: oberpar@tin.it).

elements in artery walls. Over the past decade, scientists come to appreciate a prominent role for inflammation in atherosclerosis.

Atherosclerosis develops from oxidized low-density lipoprotein (LDL) molecules. When oxidized LDL evolves in plaque formations within an artery wall, a series of reactions occur to repair the damage to the artery wall caused by oxidized LDL. The body's immune system responds to the damage to the artery wall caused by oxidized LDL by sending specialized white blood cells-macrophages (Mphs) to absorb the oxidized-LDL forming specialized foam cells. Macrophages accumulate inside arterial intima. Also, smooth muscle cells (SMC) accumulated in the atherosclerotic arterial intima, where they proliferate and secrete extracellular matrix to form a fibrous cap [1]. Unfortunately, macrophages are not able to process the oxidized LDL, and ultimately grow and rupture, depositing a larger amount of oxidized cholesterol into the artery wall. There has been considerable effort investigated LDL transport and atheroslerosis process through the artery [2]–[5]. Some authors [2] found that macrophage proliferation and constant signaling to the endothelial cells drive lesion instability, rather than an increasing influx of modified LDL. Pazos *et al*. [3] used together finite-element simulations of inflation experiments with nonlinear least-squares algorithm to estimate the material model parameters of the wall and of the inclusion. They fitted the simulated experiment and the real experiment with the parameter estimation algorithm. Hoi *et al*. [4] found that oscillatory and retrograde flow induced in the mice may exacerbate or accelerate lesion formation, but the distinct anatomical curvature of the mouse aorta is responsible for the spatial distribution of lesions. Olgac *et al*. [5] found that hypertension leads to an increased number of regions with high LDL concentration where the endothelium is represented by a three-pore model.

We are using similar approach for LDL transport through the wall domain as homogenous wall model [6]. For the moment, we did not consider multilayer wall model [7]. The Kedem–Katchalsky equations for mass transport between lumen and wall domains are used. The main difference is that we added additional reaction–diffusion equations for process of inflammation and plaque development.

This study describes a new computer model for plaque formation and development. The potential benefit for the present computational model is to simulate plaque progression based on real patient data from clinical measurements. The first section is devoted to the LDL model of transport from the lumen to

intima and a detailed 3-D model for inflammatory and process. The next section describes labeled LDL transport and matching with histological finding as well as benchmark example 3-D model of plaque formation and development. Finally, the main conclusions of the work are addressed.

II. METHODS

In this section, a continuum-based approach for plaque formation and development in 3-D is presented. All algorithms are incorporated in program PAK-Athero from the University of Kragujevac, Kragujevac [8].

The governing equations and numerical procedures are given. The blood flow is simulated by the 3-D Navier–Stokes equations, together with the continuity equation

$$-\mu\nabla^2 u_l + \rho(u_l \cdot \nabla)u_l + \nabla p_l = 0 \qquad (1)$$

$$\nabla u_l = 0 \qquad (2)$$

where u_l is the blood velocity in the lumen, p_l is the pressure, μ is the dynamic viscosity of the blood, and ρ is the density of the blood.

Mass transfer in the blood lumen is coupled with the blood flow and modeled by the convection–diffusion equation as follows:

$$\nabla \cdot (-D_l \nabla c_l + c_l u_l) = 0 \qquad (3)$$

in the fluid domain, where c_l is the solute concentration in the blood lumen and D_l is the solute diffusivity in the lumen.

Mass transfer in the arterial wall is coupled with the transmural flow and modeled by the convection–diffusion-reaction equation as follows:

$$\nabla \cdot (-D_w \nabla c_w + k c_w u_w) = r_w c_w \qquad (4)$$

in the wall domain, where c_w is the solute concentration in the arterial wall, D_w is the solute diffusivity in the arterial wall, K is the solute lag coefficient, and r_w is the consumption rate constant.

LDL transport in lumen of the vessel is coupled with Kedem–Katchalsky equations

$$J_v = L_p(\Delta p - \sigma_d \Delta \pi) \qquad (5)$$

$$J_s = P\Delta c + (1 - \sigma_f)J_v \bar{c} \qquad (6)$$

where L_p is the hydraulic conductivity of the endothelium, Δc is the solute concentration difference across the endothelium, Δp is the pressure drop across the endothelium, $\Delta \pi$ is the oncotic pressure difference across the endothelium, σ_d is the osmotic reflection coefficient, σ_f is the solvent reflection coefficient, P is the solute endothelial permeability, and $\bar{c}$ is the mean endothelial concentration.

The incremental iterative form of finite-element equations of balance is obtained by including the diffusion equations and transforming them into incremental form. The final equations are, as shown in (7) at the bottom of this page, where the matrices are

$$(\mathbf{M}_v)_{jjKJ} = \int_V \rho N_K N_J dV$$

$$(\mathbf{M}_c)_{jjKJ} = \int_V N_K N_J dV$$

$$\left(^{n+1}\mathbf{K}_{cc}^{(i-1)}\right)_{jjKJ} = \int_V DN_{K,j}N_{J,j}dV$$

$$\left(^{n+1}\mathbf{K}_{\mu v}^{(i-1)}\right)_{jjKJ} = \int_V \mu N_{K,j}N_{J,j}dV$$

$$\left(^{n+1}\mathbf{K}_{cv}^{(i-1)}\right)_{jjKJ} = \int_V N_K\, ^{n+1}c_{,j}^{(i-1)}N_J dV$$

$$\left(^{n+1}\mathbf{K}_{vv}^{(i-1)}\right)_{jjKJ} = \int_V \rho N_K\, ^{n+1}v_j^{(i-1)}N_{J,j}dV$$

$$\left(^{n+1}\mathbf{J}_{cc}^{(i-1)}\right)_{jjKJ} = \int_V \rho N_K\, ^{n+1}v_j^{(i-1)}N_{J,j}dV$$

$$\left(^{n+1}\mathbf{K}_{vp}^{(i-1)}\right)_{jjKJ} = \int_V \rho N_{K,j}\,\hat{N}_J dV$$

$$\left(^{n+1}\mathbf{J}_{vv}^{(i-1)}\right)_{jkKJ} = \int_V \rho N_K\, ^{n+1}v_{j,k}N_J dV$$

and the vectors are

$$^{n+1}\mathbf{F}_c^{(i-1)} = {}^{n+1}\mathbf{F}_q + {}^{n+1}\mathbf{F}_{sc}^{(i-1)} - \frac{1}{\Delta t}\mathbf{M}_c$$

$$\times \left\{^{n+1}\mathbf{C}^{(i-1)} - {}^n\mathbf{C}\right\} - {}^{n+1}\mathbf{K}_{cv}^{(i-1)}\left\{^{n+1}\mathbf{V}^{(i-1)}\right\}$$

$$- {}^{n+1}\mathbf{K}_{cc}^{(i-1)}\left\{^{n+1}\mathbf{C}^{(i-1)}\right\}$$

$$\left(^{n+1}\mathbf{F}_q\right)_K = \int_V N_K q^B dV \qquad {}^{n+1}\mathbf{F}_{sc}^{(i-1)}$$

$$= \int_S DN_K \nabla^{n+1}\mathbf{c}^{(i-1)} \cdot \mathbf{n}dS.$$

$$
\begin{bmatrix}
\frac{1}{\Delta t}\mathbf{M}_v + {}^{n+1}\mathbf{K}_{vv}^{(i-1)} + {}^{n+1}\mathbf{K}_{\mu v}^{(i-1)} + {}^{n+1}\mathbf{J}_{vv}^{(i-1)} & {}^{n+1}\mathbf{K}_{vp}^{(i-1)} & \mathbf{0} \\
\mathbf{K}_{vp}^{\mathbf{T}} & \mathbf{0} & \mathbf{0} \\
{}^{n+1}\mathbf{K}_{cv}^{(i-1)} & \mathbf{0} & \frac{1}{\Delta t}\mathbf{M}_c + {}^{n+1}\mathbf{K}_{cc}^{(i-1)} + {}^{n+1}\mathbf{J}_{cc}^{(i-1)}
\end{bmatrix}
$$

$$
\times \left\{\begin{matrix} \Delta\mathbf{V}^{(i)} \\ \Delta\mathbf{P}^{(i)} \\ \Delta\mathbf{C}^{(i)} \end{matrix}\right\} = \left\{\begin{matrix} {}^{n+1}\mathbf{F}_v^{(i-1)} \\ {}^{n+1}\mathbf{F}_p^{(i-1)} \\ {}^{n+1}\mathbf{F}_c^{(i-1)} \end{matrix}\right\} \qquad (7)
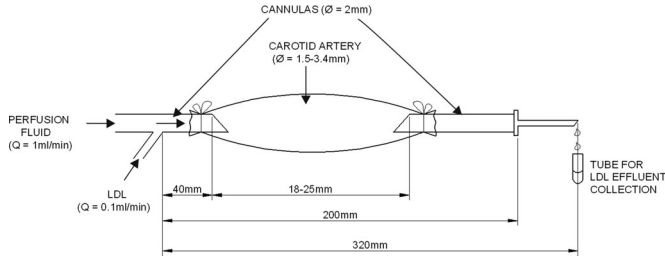$$

Fig. 1. Schematic presentation of the isolated blood vessel segment in the water bath.
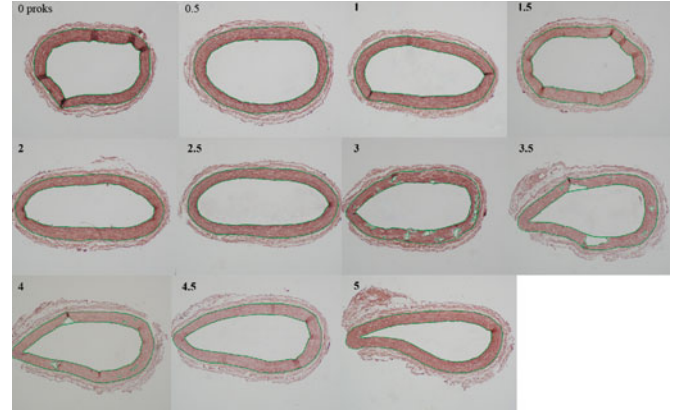

Fig. 2. Histological data (numbers on photographs indicate distances from entry carotid artery in millimeters). White zones inside media denote labeled LDL localization. Polylines around media are segmentation lines produce by image processing software.

Note that $\hat{N}_J$ are the interpolation functions for pressure (which are taken to be for one order of magnitude lower than interpolation functions N_I for velocities). The matrices $\mathbf{M}_{cc}$ and $\mathbf{K}_{cc}$ are the "mass" and convection matrices; $\mathbf{K}_{cv}$ and $\mathbf{J}_{cc}$ correspond to the convective terms of (3); and $\mathbf{F}_c$ is the force vector that follows from the convection–diffusion equation in (3) and linearization of the governing equations.

The inflammatory process was solved using three additional reaction–diffusion partial differential equations [3]

$$\partial_t Ox = d_2 \Delta Ox - k_1 Ox \cdot M$$

$$\partial_t M + \operatorname{div}(v_w M) = d_1 \Delta M - k_1 Ox \cdot M + S/(1 - S)$$

$$\partial_t S = d_3 \Delta S - \lambda S + k_1 Ox \cdot M + \gamma(Ox - Ox^{\mathrm{thr}}) \qquad (8)$$

where Ox is the oxidized LDL or c_w—the solute concentration in the wall from (4); M and S are concentrations in the intima of macrophages and cytokines, respectively; d_1, d_2, and d_3 are the corresponding diffusion coefficients; λ and γ are degradation and LDL oxidized detection coefficients; and v_w is the inflammatory velocity of plaque growth, which satisfies Darcy's law and continuity equation [9]–[12]

$$v_w - \nabla \cdot (p_w) = 0 \qquad (9)$$

$$\nabla v_w = 0 \qquad (10)$$

in the wall domain. Here, p_w is the pressure in the arterial wall.

The experimental setup analyzed LDL transport through the isolated blood vessel which was stretched to its approximate *in vivo* length. The outer diameter of the blood vessel was measured using digital camera and originally developed software. The blood vessel wall thickness was measured at the end of each experiment, using light microscope and microscopically graduated plate (see Fig. 1).

The blood vessel was considered to be viable if it contracted when 25 mM KCl was added to the bath, as well as if the presence of functional endothelium was verified by dilation with Ach (1 μM) at the end of experiment.

The isolated blood vessel was placed into the water bath with a physiological buffer. After the equilibration period (20–30 min) at a constant perfusion flow of 1 mL/min, 100 μL bolus was injected into the perfusion system containing ^{99m}Tc-Nanocis as an intravascular marker (referent tracer) or ^{125}I-LDL as a test molecule. The first 15 samples (3 drops in each sample) and 9 cumulative 3-min samples of perfusion effluent were sequentially collected. All samples were prepared for measurement of

^{125}I-LDL specific activity by addition of physiological buffer until final volume of 3 mL/sample. Measurements of perfusion effluent samples containing ^{99m}Tc-Nanocis or ^{125}I-LDL were performed by means of the gamma counter (Wallac Wizard 1400,

GMI, Inc., MN). The ^{125}I-LDL uptake is derived from the difference between the ^{99m}Tc-Nanocis value and that of ^{125}I-LDL recovery in each sample.

III. RESULTS

First, we examined LDL transport through an animal model (rabbit carotid artery) under a high blood pressure of 140 mmHg and a low perfusion flow of 1.1 mL/min.

The aim of our experiment was to determine distribution of accumulated ^{125}I-LDL radioactivity in different segments of the isolated blood vessel. Specific software for 3-D reconstruction of lumen domain and carotid wall artery was developed. A computer model of the artery is considered as a simple straight tube with deformation during a high pressure of 140 mmHg. The diameter of artery was $D = 0.0029$ m, the mean velocity $U_0 = 0.24$ m/s, dynamics viscosity $\mu = 0.0035$ Pa s, and density $\rho = 1050$ kg/m^3.

Histological images are shown in Fig. 2. The labeled LDL is localized in the white zones inside media which is probably due to destroyed radioactive LDL of tissue. Polylines around media are segmentation lines produces by in-house image processing software. Matching of histological data and computational simulation is presented in Fig. 3. The process of matching histological images was carried out by 2-D deformation of each histological cross section in order to keep the internal lumen approximately cylindrical in shape. The maximum LDL was found at distal part of the carotid artery segment at 3.5 mm from entry segment which corresponds to the largest artery diameter. This finding correlates with well-accepted research about the lowest shear stress influence. A full 3-D finite-element analysis was performed using our in-house finite-element code in order to connect the wall shear stress and function of permeability for the wall. Diagrams of wall LDL and oxidized LDL are shown
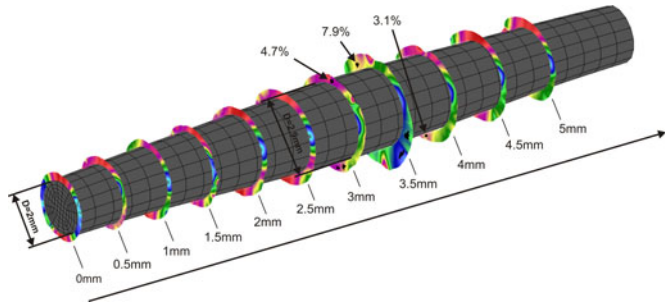
Fig. 3. Labeled LDL located in histological cross sections on each 0.5 mm for straight segment. Histological segments were obtained as deformable elastic rings opened from the current squeezed position to circle original tube. Black holes in these cross sections show location of the labeled LDL. Percentages show labeled LDL area inside media and intima wall thickness.

TABLE I
VALUES FOR RABBIT CAROTID ARTERY EXPERIMENT

Lumen	Intima	Inflammation
ρ=1000 kg/m^3		d_1=10^{-7} m^2/s
$\mu = 0.035$ [P]		d_2=10^{-7} m^2/s
D_l = 1.0e10^{-12} m^2/s	D_w = 3.0e^{-12} m^2/s	d_3=10^{-7} m^2/s
Umax=0.4m/s	r_w = -2.6x10^{-4}	k_1=1.9e^{-4} m^3/kg s
Pout=120mmHg	Pmed=100mmHg	λ=25 s^{-1}
Co=3.0x10^{-12} kg/m^3		γ = 1 s^{-1}

in Fig. 4. Experimental LDL transport of 15.7% was fitted with specific nonlinear least-squares analysis [13] in order to obtain numerical parameters. The fitted numerical parameters are given in Table I.

The following example is a benchmark example for 3-D simulation with middle stenosis of the initial 30% constriction for a time period of $t = 10^7$ s (approximately seven years). The results for velocity distribution for initial and end stages of simulations are presented in Fig. 5(a) and (b). Concentration distribution of LDL inside the lumen domain and oxidized LDL inside the intima are presented in Figs. 5 and 6. The transmural wall pressure is presented in Fig. 7. Macrophages and cytokines distributions are shown in Figs. 8 and 9. The diagram of 3-D plaque volume growing during time is given in Fig. 10. It can be seen that a change in vessel-wall volume for carotid artery quantitative corresponds to data available in the literature where the range of change in plaque volume was 247–447 mm^3 [14], From the aforementioned figures, it can be observed that with time plaque is progressing and all the variables as velocity distribution, shear stress, macrophages, cytokines are increasing. Also from Fig. 10, it can be seen that plaque progression in volume during time corresponds to clinical findings [15].

IV. CONCLUSION

Full 3-D model for plaque formation and development, coupled with blood flow and LDL concentration in blood, was created. The model is based on partial differential equations with space and times variables and it describes the biomolecular process that takes place in the intima during the initiation and the progression of the plaque.
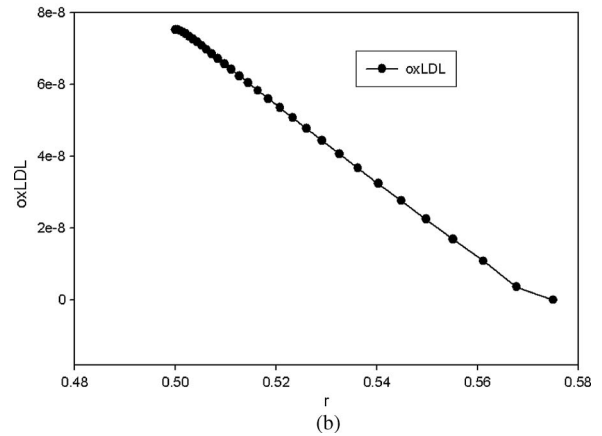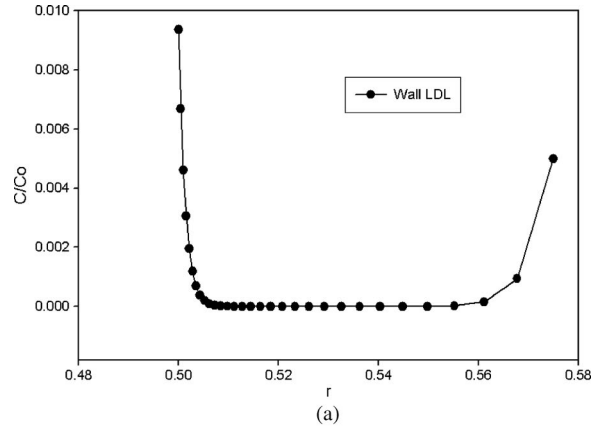

(a)

(b)

Fig. 4. Computational results. (a) Dimensionless wall LDL concentration profile in the media. b) Oxidized LDL concentration profile in the media; r is a radial position at the cross section (mm).
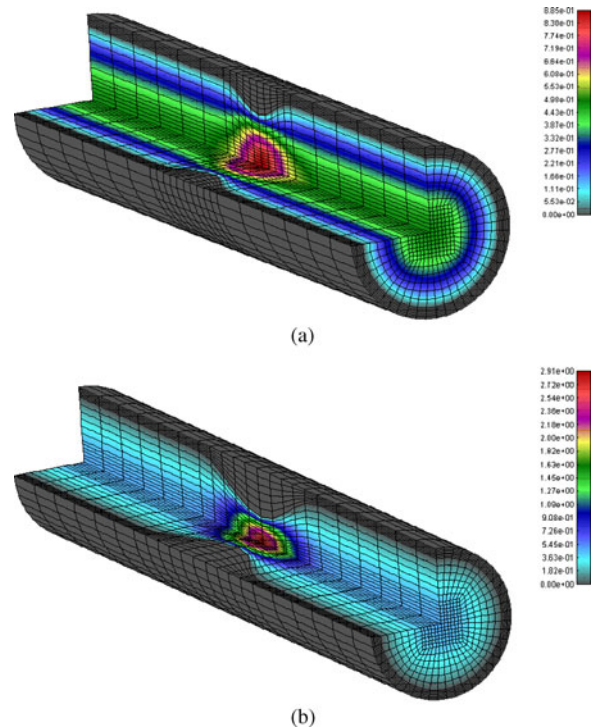

(a)

(b)

Fig. 5. (a) Velocity distribution for an initial mild stenosis 30% constriction by area. (b) Velocity distribution at the end of stenosis process after 10^7 s (units m/s).
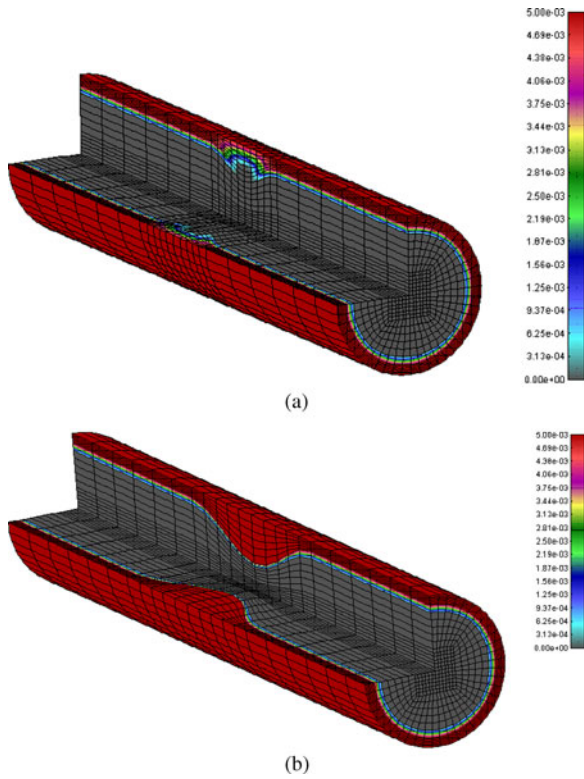
Fig. 6. (a) Oxidized LDL distribution in the intima for an initial mild stenosis 30% constriction by area. (b) Oxidized LDL distribution in the intima at the end of stenosis process after 10^7 s (units mg/mL).

Fig. 8. (a) Macrophages distribution in the intima for an initial mild stenosis 30% constriction by area. (b) Macrophages distribution in the intima at the end of stenosis process after 10^7 s (units mg/mL).
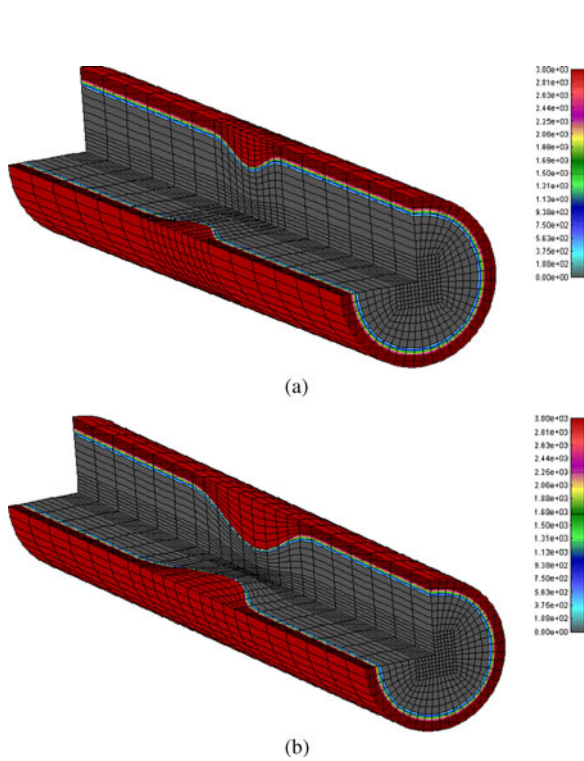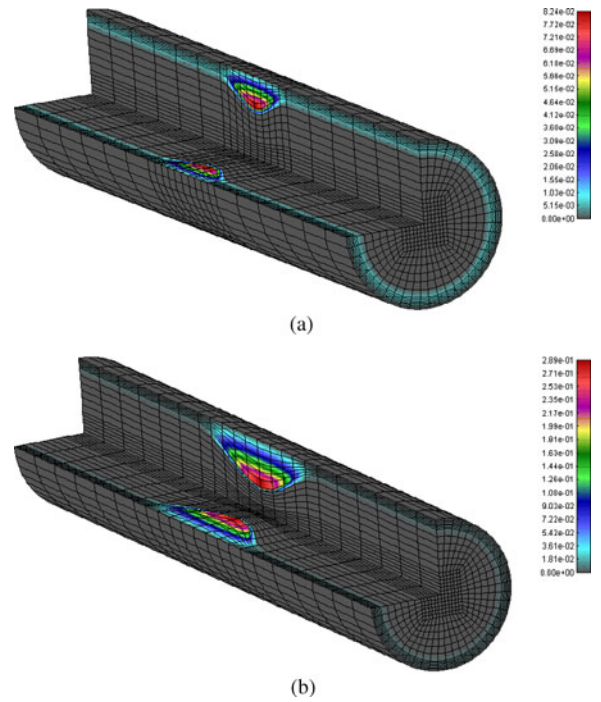

Fig. 7. (a) Intima wall pressure distribution for an initial mild stenosis 30% constriction by area. (b) Intima wall pressure distribution at the end of stenosis process after 10^7 s (units Pa).
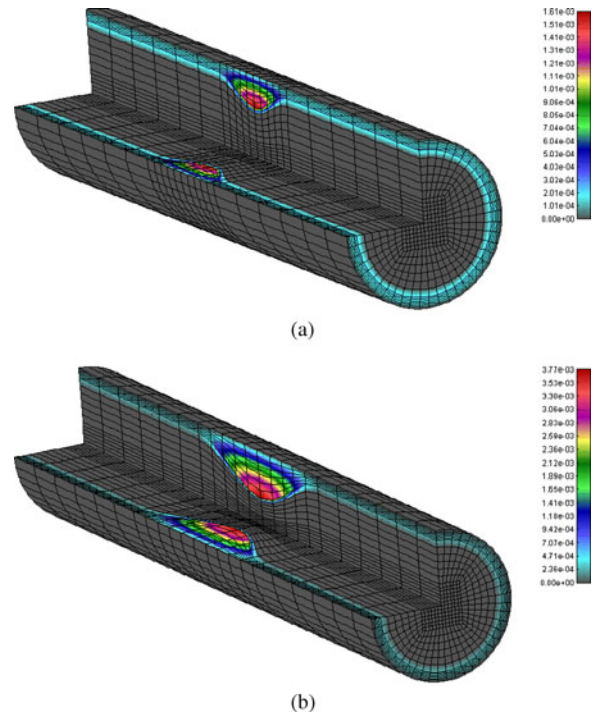

Fig. 9. (a) Cytokines distribution in the intima for an initial mild stenosis 30% constriction by area. (b) Cytokines distribution in the intima at the end of stenosis process after 10^7 s (units mg/mL).
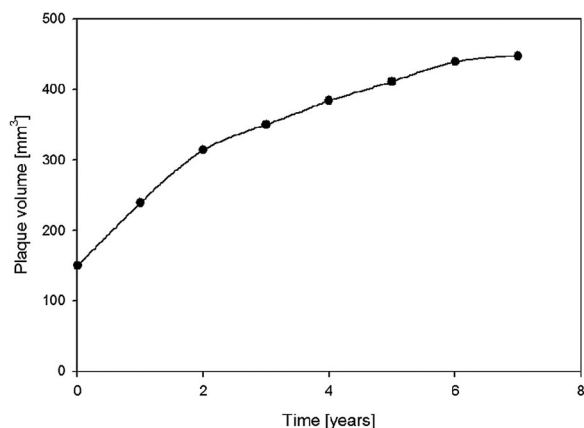
Fig. 10.   Plaque progression during time (computer simulation).

The current computational model is initial demonstration of very complex atherosclerotic process and has some limitations. First of all, the arteries in the human body are not of the same embryological origin and, therefore, might react differently. Plaque components of the wall measured from the medical images should be included in the model. Also, quantification of the real patient-specific plaque progression has to be investigated. Fluid–structure interaction should be included.

Determination of plaque location and progression in time for a specific patient show a potential benefit for future prediction of this vascular disease using computer simulation. The understanding and the prediction of the evolution of atherosclerotic plaques either into vulnerable plaques or into stable plaques are major tasks for the medical community.

REFERENCES

[1] J. Loscalzo and A. I. Schafer, *Thrombosis and Hemorrhage*, 3rd ed. Philadelphia, PA: Williams & Wilkins, 2003.

[2] A. Ougrinovskaia, R. S. Thompson, and M. R. Myerscough, "An ODE model of early stages of atherosclerosis: Mechanisms of the inflammatory response," *Bull Math. Biol.*, vol. 72, no. 6, pp. 1534–61, 2010.

[3] V. Pazos, R. Mongrain, and J. C. Tardif, "Mechanical characterization of atherosclerotic arteries using finite-element modeling: Feasibility study on mock arteries," *IEEE Trans. Biomed. Eng.*, vol. 57, no. 6, pp. 1520–1528, Jun. 2010.

[4] Y. Hoi, Y. Q. Zhou, X. Zhang, R. M. Henkelman, and D. A. Steinman, "Correlation between local hemodynamics and lesion distribution in a novel aortic regurgitation murine model of atherosclerosis," *Ann. Biomed. Eng.*, vol. 39, no. 5, pp. 1414–1422, 2011.

[5] U. Olgac, D. Poulikakos, S. C. Saur, H. Alkadhi, and V. Kurtcuoglu, "Patient-specific three-dimensional simulation of LDL accumulation in a human left coronary artery in its healthy and atherosclerotic states," *Amer. J. Physiol. Heart Circ. Physiol.*, vol. 296, no. 6, pp. 1969–1982, 2009.

[6] N. Sun, N. B. Wood, A. D. Hughes, S. A. M. Thom, and X. Y. Hu, "Fluid-wall modelling of mass transfer in an axisymmetric stenosis: Effects of shear-dependent transport properties," *Ann. Biomed. Eng.*, vol. 34, no. 7, pp. 1110–1128, 2006.

[7] N. Sun, N. B. Wood, A. D. Hughes, S. A. M. Thom, and X. Y. Hu, "Effects of transmural pressure and wall shear stress on LDL accumulation in the arterial wall: A numerical study using a multi-layered model," *Amer. J. Physiol. Heart Circ. Physiol.*, vol. 292, pp. 3148–3157, 2007.

[8] N. Filipovic, N. Meunier, and M. Kojic, "PAK-Athero, specialized three-dimensional PDE software for simulation of plaque formation and development inside the arteries," University of Kragujevac, Kragujevac, Serbia, 2010.

[9] M. Kojic, N. Filipovic, B. Stojanovic, and N. Kojic, *Computer Modeling in Bioengineering—Theoretical Background, Examples and Software*. Chichester, U.K: Wiley, 2008.

[10] N. Filipovic and M. Kojic, "Computer simulations of blood flow with mass transport through the carotid artery bifurcation," *Theor. Appl. Mech. (Serbian)*, vol. 31, no. 1, pp. 1–33, 2004.

[11] N. Filipovic, S. Mijailovic, A. Tsuda, and M. Kojic, "An implicit algorithm within the arbitrary Lagrangian–Eulerian formulation for solving incompressible fluid flow with large boundary motions," *Comp. Meth. Appl. Mech. Eng.*, vol. 195, no. 44-47, pp. 6347–6361, 2006.

[12] N. Filipovic, M. Kojic, M. Ivanovic, B. Stojanovic, L. Otasevic, and V. Rankovic, MedCFD, *Specialized CFD software for simulation of blood flow through arteries*, Kragujevac, Serbia, University of Kragujevac, 2006.

[13] C. Guy, *Nonlinear Least Squares for Inverse Problems, Nonlinear Least Squares for Inverse Problems Theoretical Foundations and Step-by-Step Guide for Applications*, 2nd ed.   New York: Springer, 2010.

[14] L. Boussel, S. Arora, J. Rapp, B. Rutt, J. Huston, D. Parker, C. Yuan, H. Bassiouny, and D. Saloner, "Atherosclerotic plaque progression in carotid arteries: Monitoring with high-spatial-resolution MR imaging—Multicenter trial," *Radiology*, vol. 252, no. 3, pp. 789–796, 2009.

[15] V. Calvez, A. Ebde, N. Meunier, and A. Raoult, "Mathematical modelling of the atherosclerotic plaque formation," in *Proc. Eur. Series in Appl. and Industrial Math.*, 2008, vol. 28, pp. 1–12.

Nenad Filipovic (M'10) received the Ph.D. in bioengineering from the University of Kragujevac, Kragujevac, Serbia, in 1999.

He was a Research Associate at Harvard School of Public Health, Boston, MA. He is currently a Professor in bioengineering at Faculty of Mechanical Engineering, University of Kragujevac. He is the author or coauthor of 6 textbooks and 1 monography, and of more than 180 publication, from more than 50 scientific papers in peer-reviewed journals. He is an author of several types of software for modeling with finite-element method and discrete methods from fluid mechanics and multiphysics, as well as connection of medical data with mechanics solvers. His research interest includes computer modeling in bioengineering.

Mirko Rosic received the M.D. degree from the University of Kragujevac, Kragujevac, Serbia, in 1982.

He is a Professor of physiology at Faculty of Medicine, University of Kragujevac, Kragujevac, Serbia, where he was a Dean. He leads the Laboratory for biomedical research. He was an honorary Lecturer at St. Thomas's Medical Faculty in London. He has authored more than 120 scientific publications as well as edited and coauthored 9 text books. His research interests include cardiovascular physiology and experimental research.

Irena Tanaskovic completed Integrated Academic Studies for a Doctor of Medicine at Medical Faculty, University of Kragujevac, Kragujevac, Serbia in 1999. She received the academic title of a specialist in cytology, histochemistry, electron microscopy, and embryology at University of Belgrade School of Medicine, Belgrade, Serbia, in 2003. She received the Ph.D. degree in histology and embryology from the University of Kragujevac in 2006.

She is currently an Assistant Professor of histology and embryology at Faculty of Medicine and Faculty of Dentistry, University of Kragujevac. Her research interests include vascular histology, embryology, and cell biology.

Zarko Milosevic received the Graduate's degree from the Faculty of Mechanical Engineering, University of Kragujevac, Kragujevac, Serbia, in 2009. He is currently working toward the Ph.D. degree at the same institution and working as a Research Associate at Bioengineering Research and Development Center, BIOIRC, Kragujevac.

His research interests include software engineering and computer modeling in bioengineering.

Milos R. Kojic received the Ph.D. degree in mechanical engineering from Rice University, Houston, TX, in 1972.

He is currently a Visiting Professor at The Methodist Hospital Research Institute, Houston.

Dalibor Nikolic received the Graduate's degree from the Faculty of Mechanical Engineering, University of Kragujevac, Kragujevac, in 2011. He is currently working toward the Ph.D. degree at the same institution and is working as a Research Assistant at Bioengineering Research and Development Center for Bioengineering, BIOIRC, Kragujevac.

His research interest includes computer modeling of medical problems.

Dimitrios I. Fotiadis (M'01–SM'06) received the Diploma degree in chemical engineering from the National Technical University of Athens, Athens, Greece, in 1985, and the Ph.D. degree in chemical engineering and materials Science from the University of Minnesota, Twin Cities, Minneapolis, MN, in 1990.

He is currently a Professor of biomedical engineering in the Department of Materials Science and Engineering, University of Ioannina, Ioannina, Greece; the Director of the Unit of Medical Technology and Intelligent Information Systems, Department of Materials Science and Engineering; and an Affiliated Member of FORTH, Biomedical Research Institute. He was a Visiting Researcher at the RWTH, Aachen, Germany, and the Massachusetts Institute of Technology, Boston, MA. He has published more than 140 papers in scientific journals, 270 papers in peer-reviewed conference proceedings, and more than 25 chapters in books. He is the Editor of 16 books. His research interests include modeling of human tissues and organs, intelligent wearable devices for automated diagnosis, and bioinformatics. His work has received more than 1500 citations.

Dr. Fotiadis is an Associate Editor of the IEEE TRANSACTIONS ON INFORMATION TECHNOLOGY IN BIOMEDICINE.

Nebojsa Zdravkovic received the Ph.D. degree in bioengineering from the University of Kragujevac, Kragujevac, Serbia, in 2000.

He is currently a Professor of medical statistics at Faculty of Medicine, University of Kragujevac. His research interests include data mining, statistics, and computer modeling.

Aleksandar Peulic received the Diploma degree in electronic engineering and the Master of Science degree in electrical engineering both from the Faculty of Electronic Engineering, University of Nis, Nis, Serbia, in 1994 and 2004, respectively.

He is an Assistant Professor at Technical Faculty Cacak, University of Kragujevac, Cacak, Serbia. He was a Postdoctoral Research Fellow at the University of Alabama, Huntsville, in 2008. His research interests include microcontrollers systems, wearable sensors, and bioengineering.

Oberdan Parodi received the M.D. degree from the University of Pisa, Pisa, Italy, in 1972.

He was a Visiting Professor at University of California, Los Angeles, during 1983–84. He is currently the Director of Department of Cardiology, CNR Clinical Physiology Institute,, Niguarda Hospital, Milan, Italy. His research interests include cardiac imaging, coronary blood flow, and myocardial remodeling in heart failure.